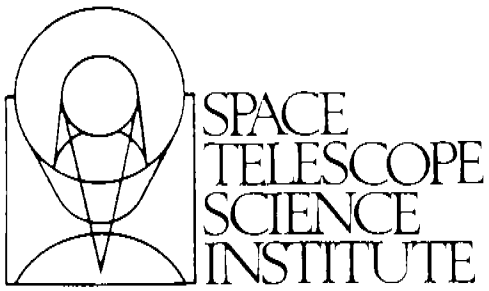

INSTRUMENT SCIENCE REPORT

CAL/FOS-032

TITLE: AN AUTOMATED METHOD FOR COMPUTING ABSOLUTE INSTRUMENTAL SENSITIVITY CURVES FOR FOS: RESULTS OF TESTING WITH IUE SPECTRA

AUTHOR: D. Lindler and R. Bohlin

DATE: August 1986

ABSTRACT

A method for computing inverse sensitivity curves for the Faint Object Spectrograph (FOS) is investigated by deriving the calibration of the International Ultraviolet Explorer (IUE). The method involves a progressive polynomial fitting technique, which will generate a smooth sensitivity curve from the raw ratio of the flux in the standard star spectrum to the counts per sec in the observed spectrum. The "smoothness" of the fitted curves are comparable to the present IUE sensitivity curves, which were created by manually drawing a curve through the raw data.

DISTRIBUTION:

ISB

CSC

SDAS

SOGS

IDT

I. INTRODUCTION

The goal of absolute flux calibration is to compute the inverse sensitivity function $S^{-1}(\lambda)$ which satisfies

$$F(\lambda) = D(\lambda)\ S^{-1}(\lambda),$$

where $F(\lambda)$ is the absolute flux of the source and $D(\lambda)$ is the observed, linearized counts for FOS; or in the case of IUE, $D(\lambda)$ is the linearized response in Flux Number (FN) units. An obstacle to computing S^{-1} from the ratio F/D is that $D(\lambda)$ and $F(\lambda)$ are tabular functions with different resolutions and sample spacing. This paper describes techniques for computing and smoothing the ratio into a suitable inverse sensitivity curve.

II. METHOD

Compute the inverse sensitivity from an observation $D(\lambda$ and the complete absolute flux distribution for the standard spectrum $F(\lambda)$ using the following five steps:

1) If the resolution of the standard star spectrum and the observed spectrum differ significantly, the ratio will show structure in the vicinity of spectral features. To produce a smoother ratio F/D, convolve the higher resolution spectrum with the observed spectral point-spread-function (PSF) of the lower resolution spectrum before dividing. To be precise, each spectrum should be convolved with the PSF of the other spectrum.

2) Convert $D(\lambda)$ and $F(\lambda)$ to the same wavelength scale by one of four options:

   a) Interpolate $D(\lambda)$ to match the scale for $F(\lambda)$.

   b) Interpolate $F(\lambda)$ to match the scale for $D(\lambda)$.

   c) Integrate $D(\lambda)$ to match the sample spacing and specified resolution of $F(\lambda)$.

   d) Integrate $F(\lambda)$ to match the sample spacing and specified resolution of $D(\lambda)$.

   e) Integrate both $F(\lambda)$ and $D(\lambda)$ into bins of a specified wavelength interval.

In both a) and b) linear interpolation is used and in c) and d) trapezoidal integration is used. In most cases, method d) is the most appropriate. Method a) and b) can be used, if the sampling intervals for $D(\lambda)$ and $F(\lambda)$ are similar. Method c) is used for the FOS prism, where the extreme nonlinearity of the wavelength scale makes a constant wavelength bin size inappropriate. If method d) is used and if the wavelength bin

size is much larger than the resolution element of $F(\lambda)$ and of $D(\lambda)$, then step one can be ignored.

3) Compute the ratio $C(\lambda) = \log F(\lambda)/D(\lambda)$

4) Smooth $C(\lambda)$ using the following algorithm:

At each data point i in C, fit a low order polynomial of order m through points $i-(n-1)/2$ to $i+(n-1)/2$ where m and n are selectable parameters. Let $C'(i)$ be the value of the polynomial at point i.

5) Compute $S^{-1}(\lambda) = 10^{C'(\lambda)}$

If noise causes values of zero in $D(\lambda)$ from step 2, the ratio in step 3 can be computed from $D(\lambda)/F(\lambda)$. The reciprocal of the sensitivity curve computed in step 5 will give the inverse sensitivity.

The users guide to the software that implements steps 1-5 is Appendix A.

III. CALIBRATION OF IUE

To evaluate the algorithm described above, a calibration of three cameras on IUE was performed. The calibration of IUE SWP and LWR response in FN was done using OAO 2 absolute flux distributions as standards after the correction of the OAO 2 flux scale according to Bohlin and Holm (1984). The LWP camera was then calibrated using absolutely calibrated LWR spectra as the standards.

a) IUE SWP CALIBRATION

The IUE SWP camera was calibrated using OAO 2 data for the stars μ Col, ζ Cas, η Aur, λ Lep, 10 Lac, and η UMa. Multiple observations of each star, as specified by Bohlin and Holm (1984), were averaged to give the mean IUE response in flux numbers FN resampled to a 1.18Å spacing between points. All IUE FN values are appropriate for point sources in the large IUE aperture. If the wavelength scales for $D(\lambda)$ or $F(\lambda)$ are imprecise, spurious features in the ratio will arise in the regions of spectral lines. To reduce the scatter of values in the ratio of OAO 2 to IUE data, wavelength corrections were derived from the assumption that the strong Lα feature is at 1215.7Å. The following corrections to the archival wavelength scales were applied:

	IUE	OAO 2
μ Col	1.1Å	-5.0Å
ζ Cas	-0.1	-2.0
η Aur	2.6	-3.6
λ Lep	0.6	-3.2
10 Lac	-1.4	-0.6
η UMa	2.8	-3.0

The IUE inverse sensitivity was derived according to the method of Section II as follows:

For step 1, a 13 point mean filter was applied to the IUE data to approximately match the resolution of the OAO data after deriving the wavelength shifts. The value of 13 points (15Å) was determined empirically by visual comparison of the OAO 2 spectra with IUE data smoothed by different size filters. Figure 1 shows the comparison of IUE data for one star calibrated with the IUE inverse sensitivity curve of Bohlin (1986), smoothed with a 13 point mean filter, and compared to the OAO 2 data.

For step 2, the IUE and OAO 2 data were converted to the same wavelength scale by integrating both into 5Å bins. The log of the ratio for each of the 6 stars was taken (step 3) and smoothed using 4th order polynomials (m = 4) of width n = 65 data points (step 4). Figure 2 shows the average of the smooth curves for all 6 stars with the ratios from step 3 of all stars overplotted as points. Figure 3 shows a comparison of the curve with the IUE inverse sensitivity curve for point sources in the large aperture from Bohlin (1986).

The ratio of the two curves in Figure 4 show agreement to 4% longward of Lα. Most of the deviation from unity in Figure 4 is due to the fact that Bohlin (1986) revised the IUE calibration to make the fluxes internally consistent among the three modes, while requiring the point source combination of large and small aperture spectra to remain unchanged for five well observed stars. Since the IUE spectra used to create Figure 4 are heavily weighted to trailed spectra, the deviation from unity reflects the trailed sensitivity of Bohlin (1986) that was necessary for internal consistency. Thus, the deviations from unity in Figure 4 could be used to correct the external IUE calibration by applying those corrections uniformly to all three modes: trailed and point sources in either aperture. While Bohlin was aware of this problem, he considered the changes required to the external calibration to be too small compared to the external error bar of 10% to justify a change.

Two factors must be considered in evaluating the smoothing techniques. First, the computed calibration curve of Figure 3

should be smooth (i.e. not show any small scale granularity); and second, it should follow the data. Smoothness is a constraint imposed by the expected physical properties of the optics. Any true, small scale granularity in the sensitivity of the detector should be removed by an independent flat field correction. Figure 5 shows the normalized second difference of the computed curve and the IUE curve. The normalized second difference is the difference between each point and the average of its two neighbors, all divided by the value of the data point. The results indicate that the granularity over the 5Å data point separation is typically 0.3%.

To evaluate how well the smoothing technique followed the raw data, the IUE data was calibrated with the computed sensitivity curve, smoothed to the OAO 2 resolution, and compared to the OAO 2 fluxes. Figure 6 shows the ratios of the IUE absolutely calibrated data to the OAO 2 reference spectra in 5Å bins (plotted as points). The average ratio and standard deviation in the ratio for the six stars were computed; and the average plus one sigma and the average minus one sigma error are overplotted as solid lines. For the most part, the expected ratio of 1.0 lies between the one sigma error estimates.

b) IUE LWR CALIBRATION

The process was repeated for the LWR camera using stars, μ Col, ζ Cas, η Aur, 10 Lac, and η UMa. Due to the lack of a good wavelength fiducial, no correction to the wavelength scales was performed. However, the lack of sharp spectral features means that wavelength inaccuracies have minimal effect on the results.

For the LWR, data was integrated in 10Å bins to match the separation of data points in the OAO 2 data in the LWR wavelength range. The sensitivity was derived using 4th order polynomials ($m = 4$) over $n = 35$ data points to find smooth fits to the ratios. Figures 7-11 show the analysis for LWR that corresponds to the results for SWP in Figures 2-6. The 50Å period that appears in Figure 10 for the LWR calibration of Bohlin is caused by a combination of the coarse 50Å separation between the tabulated points, by the steepness of the IUE calibration, and by the unsophisticated logarithmic interpolation over the 50Å separations. Since the discontinuities in slope are always less than 1%, there are probably no applications where the effect is important.

c) IUE LWP CALIBRATION

By adopting the LWR absolute fluxes for the first year of IUE operations, the IUE LWP camera can be calibrated from the LWR camera using the standard star fluxes for BD+75°325, BD+28°4211, HD60753, and HD93521 from Bohlin (1986). Linear interpolation can be used to bring the LWR spectra onto the same wavelength scale as the LWP spectra, since both cameras have approximately the same resolution and sampling interval. Thus, step 1 of the

algorithm is skipped, while step 2b is used. In step 4, m = 4 and n = 175. The LWP data consisted of an average of trailed spectra and point source spectra from both the large and small apertures. Thus, the final computed inverse sensitivity curve is an average curve for the three modes of operation. Because of the well known difference in sensitivity among these three modes for SWP and LWR (Bohlin 1986) and for LWP (Harris and Cassatella 1985), the average calibration is inappropriate for spectra purely from any one mode.

Figures 12 through 16 show the results for the LWP camera. Figure 12 shows more noise than Figure 7, since the sampling is reduced to 1.87Å from 10Å. Figure 13 shows deviations from a smooth curve in the IUE inverse sensitivity curve of Cassatella and Harris (1983) around 2800Å which do not show up in the computed curve; and Figure 14 indicates that the IUE sensitivity curve of Cassatella and Harris is approximately 4% high on average. Figure 15 shows the fine scale structure of the curves with the 50Å pattern present as for LWR. Figure 16 indicates that the curve fitting technique did an excellent job of following the raw data.

IV. SUMMARY

An algorithm for finding FOS calibrations for the 8 useful dispersion modes on each detector has been developed and proven for IUE, which is the most relevant data set available and should represent a worst case in comparison to the high signal-to-noise data expected for FOS. The IUE results are directly relevant to the in-flight calibration of FOS, since IUE standards will play the role of OAO 2 spectra in this work.

For the SWP and LWR cameras on IUE, the calibrations have a smoothness comparable to the hand drawn, existing IUE calibrations. The accuracy of the algorithm in tracking the mean calibration implied by the average of the set of standard stars is somewhat better than for the calibration of Bohlin (1986), as tabulated below.

RESIDUAL ERROR BETWEEN AVERAGE RATIO
OF IUE TO OAO 2 FLUXES

	SWP	LWR
Bohlin (1986)	2.5	2.2
This Work	2.0	1.5

The values above are in percent and are calculated (for the example of SWP) by averaging the 6 points at each wavelength bin of Figure 6, finding the absolute value of the difference from unity, and then averaging over all wavelength bins. The

improvement to the fit of less than 1% does not justify any change to the calibration of Bohlin (1986) for SWP and LWR.

In the case of the LWP camera, the analysis documented in Figures 12-16 suggests that the calibration for LWP in Table 1 may be a significant improvement over the Cassatella and Harris (1983) results, in a case such as the IUE program to get flux standards for HST where the spectra are averages of trailed and point source spectra. However, both results should be regarded as preliminary and approximate for two reasons:

1. The LWP linearity correction (ITF) has only a single image per level. Serious absolute calibration work should await the implementation of the new ITF with four images per level, if that event and the required reprocessing of calibration spectra preceeds HST launch.

2. The LWP calibration for the three observing modes is known to differ significantly (Harris and Cassatella 1985), in analogy to the differences found among the modes for SWP and LWR by Bohlin (1986). The LWP calibration in Table 1 represents an average for four stars with a total of 6 trailed spectra, 28 large aperture point source spectra, and 6 small aperture spectra.

REFERENCES

Bohlin, R.C., and Holm, A.V. 1984, NASA IUE Newsletter, 24, 74; 1984, ESA IUE Newsletter, 20, 22.

Bohlin, R.C. 1986, Ap. J., 308, Sept. 15.

Cassatella, A., and Harris, A. W. 1983, ESA IUE Newsletter, 17, 12; NASA IUE Newsletter, 23, 21.

Harris, A.W., and Cassatella, A. 1985, ESA IUE Newsletter, 22, 9.

TABLE 1

AN INTERIM ABSOLUTE CALIBRATION FOR THE LWP CAMERA

λ (Å)	Change[a]	S^{-1} (10^{-14} erg cm^{-2} $Å^{-1}$ FN^{-1})
1850	.967	16.8 :
1900	1.103	5.61
1950	1.016	3.06
2000	1.061	2.28
2050	1.020	2.00
2100	1.048	1.89
2150	1.036	1.93
2200	1.048	1.89
2250	1.040	1.73
2300	1.007	1.49
2350	1.033	1.23
2400	1.040	1.00
2450	1.053	.835
2500	1.059	.700
2550	1.024	.615
2600	1.021	.566
2650	.979	.525
2700	1.022	.492
2750	1.044	.481
2800	1.020	.492
2850	1.062	.520
2900	.993	.570
2950	.994	.656
3000	.995	.799
3050	1.059	1.02
3100	1.072	1.38
3150	1.069	2.03
3200	1.120	2.99
3250	1.160	4.93
3300	1.151	9.20
3350	.997	15.5 :

[a]Ratio of the S^{-1} of Cassatella and Harris to the interim calibration in the next column.

FIGURE CAPTIONS

Fig. 1. - A comparison of the OAO-2 spectrum of μ Col (dotted line) and the IUE spectrum (solid line) smoothed with a 13 point mean filter. The absolute calibration of the IUE data is based on the Bohlin (1986) inverse sensitivity curve.

Fig. 2. - The results of the curve fitting for the IUE SWP camera. The dots show the raw inverse sensitivity in 5Å bins for all six stars, and the solid line shows the fitted curve.

Fig. 3. - A comparison of the IUE sensitivity curve of Bohlin (dotted line) versus the computed curves for the SWP camera.

Fig. 4. - The ratio of the computed sensitivity curve to the large aperture point source sensitivity of Bohlin (1986) for the SWP camera on IUE. The difference between the two results are well within the quoted errors of 10% longward of Lα.

Fig. 5. - The normalized second differenced of the computed SWP curve and the IUE sensitivity curve of Bohlin (offset by +0.01). The second difference for data point d_i is computed by $[d_i-(d_{i-1}+d_{i+1})/2]/d_i$. Both curves are smooth to a fraction of a percent.

Fig. 6. - The dots show the ratio over 5Å bins of the IUE SWP data calibrated with the new sensitivity curve, smoothed to the OAO 2 resolution, and compared to the OAO 2 data for six stars. The average ratio plus 1σ and the average ratio minus 1σ for the six stars are the solid lines.

Fig. 7. - Same as Figure 2 for the LWR camera. Five stars were used with 10Å bins for each data point.

Fig. 8. - Same as Figure 3 (LWR camera).

Fig. 9. - Same as Figure 4 (LWR camera).

Fig. 10. - Same as Figure 5 (LWR camera).

Fig. 11. - Same as Figure 6 (LWR camera), except that the bins are 10Å wide. The clump of points above the 1σ error limit below 2000Å are for μ Col and indicate some problem with those data.

Fig. 12. - The results of the curve fitting for the LWP camera. The dots show the raw ratios of 4 stars. The reference spectra (LWR) were interpolated to the LWP wavelength scale. The solid line shows the fitted curve.

Fig. 13. - Same as Figure 3 (LWP camera), except that the LWP calibration (dashed line) is attributed to Cassatella and Harris (1983).

Fig. 14. - Ratio of the calibration for LWP found here to the calibration of Cassatella and Harris (1983). Both calibrations are for an arbitrarily selected set of spectra from the three observing modes.

Fig. 15. - Same as Figure 5 (LWP camera).

Fig. 16. - Same as Figure 6 (LWP camera), except that the integration bins are 10 Å wide and the comparison is with the IUE data from LWR instead of with OAO 2.

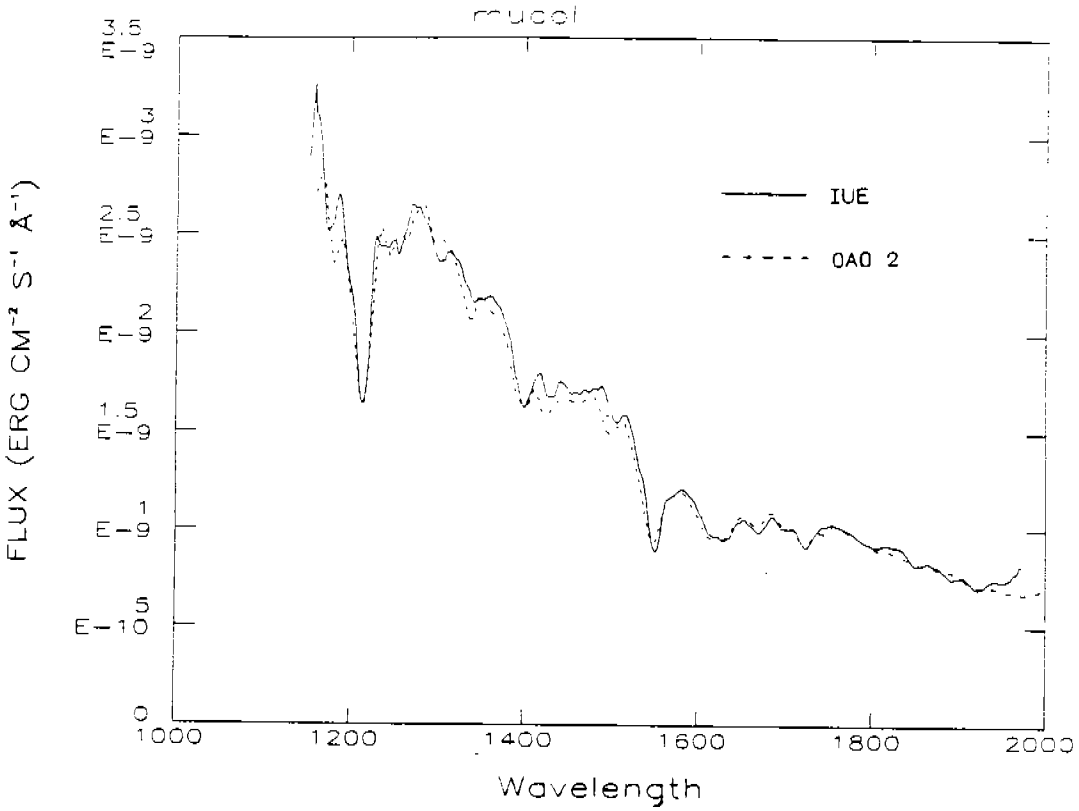
mucol
FLUX (ERG CM⁻² S⁻¹ Å⁻¹)
3.5 E-9
E-9
2.5 E-9
2 E-9
1.5 E-9
1 E-9
5 E-10
0
1000
1200
1400
1600
1800
2000
Wavelength
IUE
OAO 2

Fig. 1

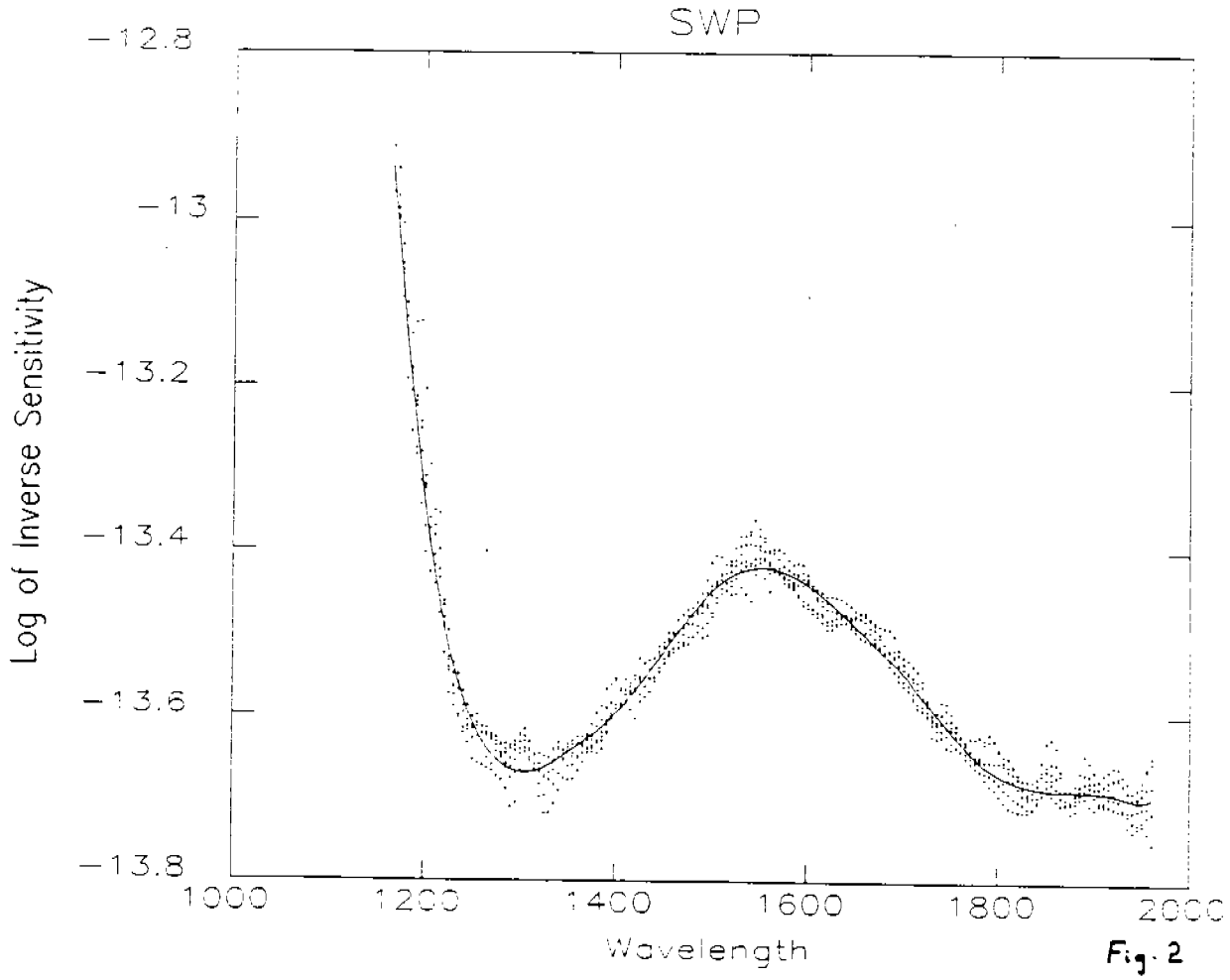
SWP
Log of Inverse Sensitivity
-12.8
-13
-13.2
-13.4
-13.6
-13.8
1000
1200
1400
1600
1800
2000
Wavelength

Fig. 2

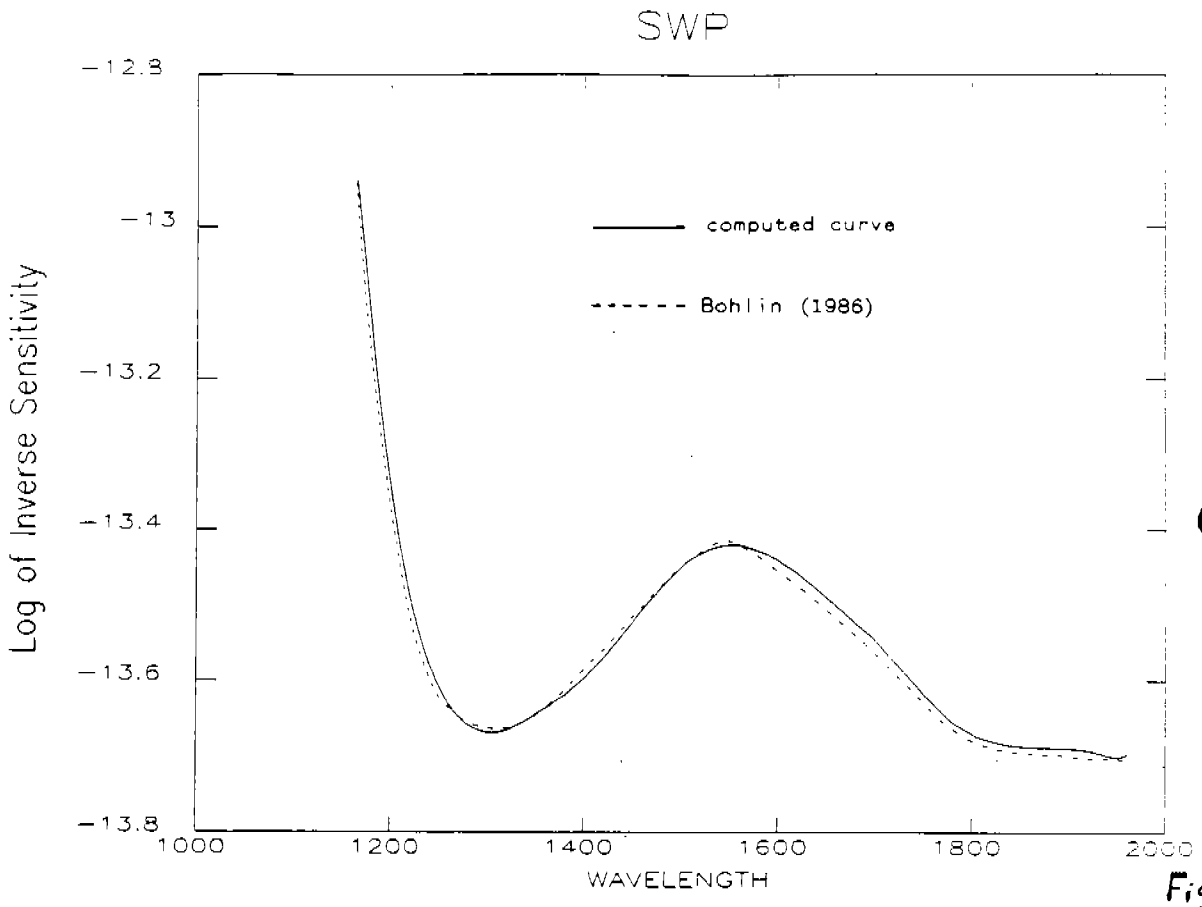
SWP
−12.8
−13
−13.2
−13.4
−13.6
−13.8
Log of Inverse Sensitivity
computed curve
Bohlin (1986)
1000
1200
1400
1600
1800
2000
WAVELENGTH

Fig. 3

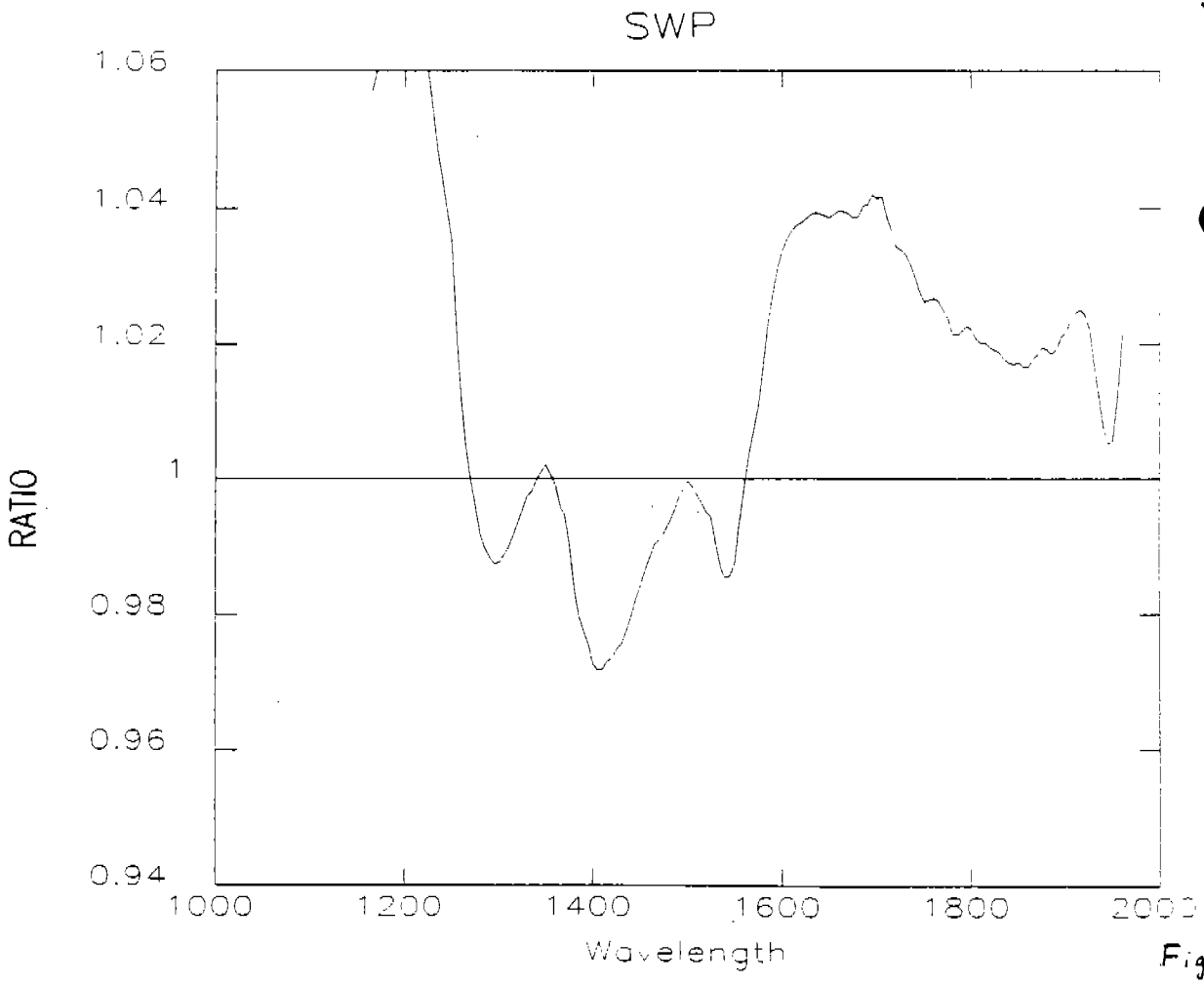
SWP
1.06
1.04
1.02
1
0.98
0.96
0.94
RATIO
1000
1200
1400
1600
1800
Wavelength

Fig. 4

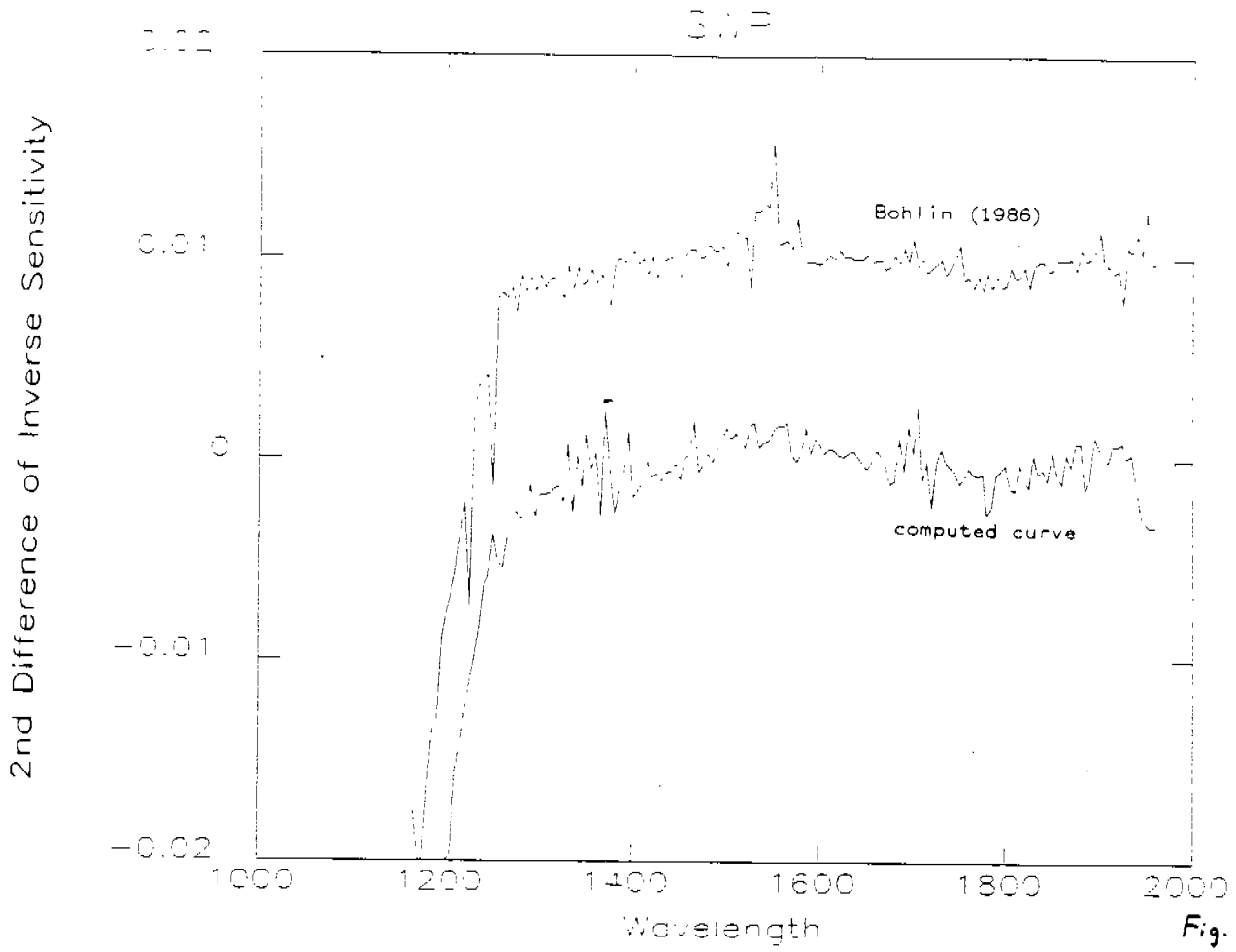
2nd Difference of Inverse Sensitivity
0.02
0.01
0
−0.01
−0.02
Bohlin (1986)
computed curve
1000
1200
1400
1600
1800
2000
Wavelength

Fig. 5

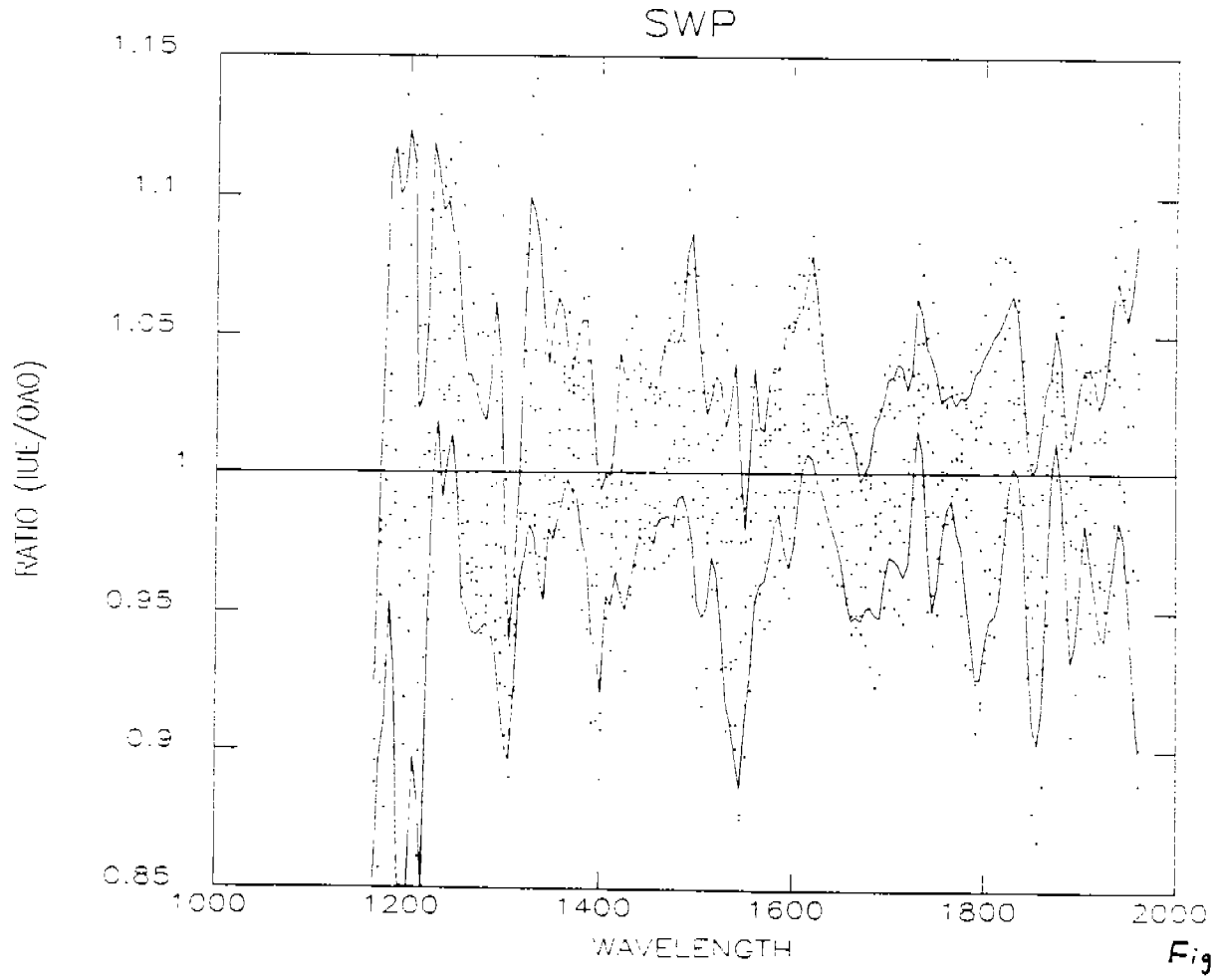
SWP
RATIO (IUE/OAO)
1.15
1.1
1.05
1
0.95
0.9
0.85
1000
1200
1400
1600
1800
2000
WAVELENGTH

Fig. 6

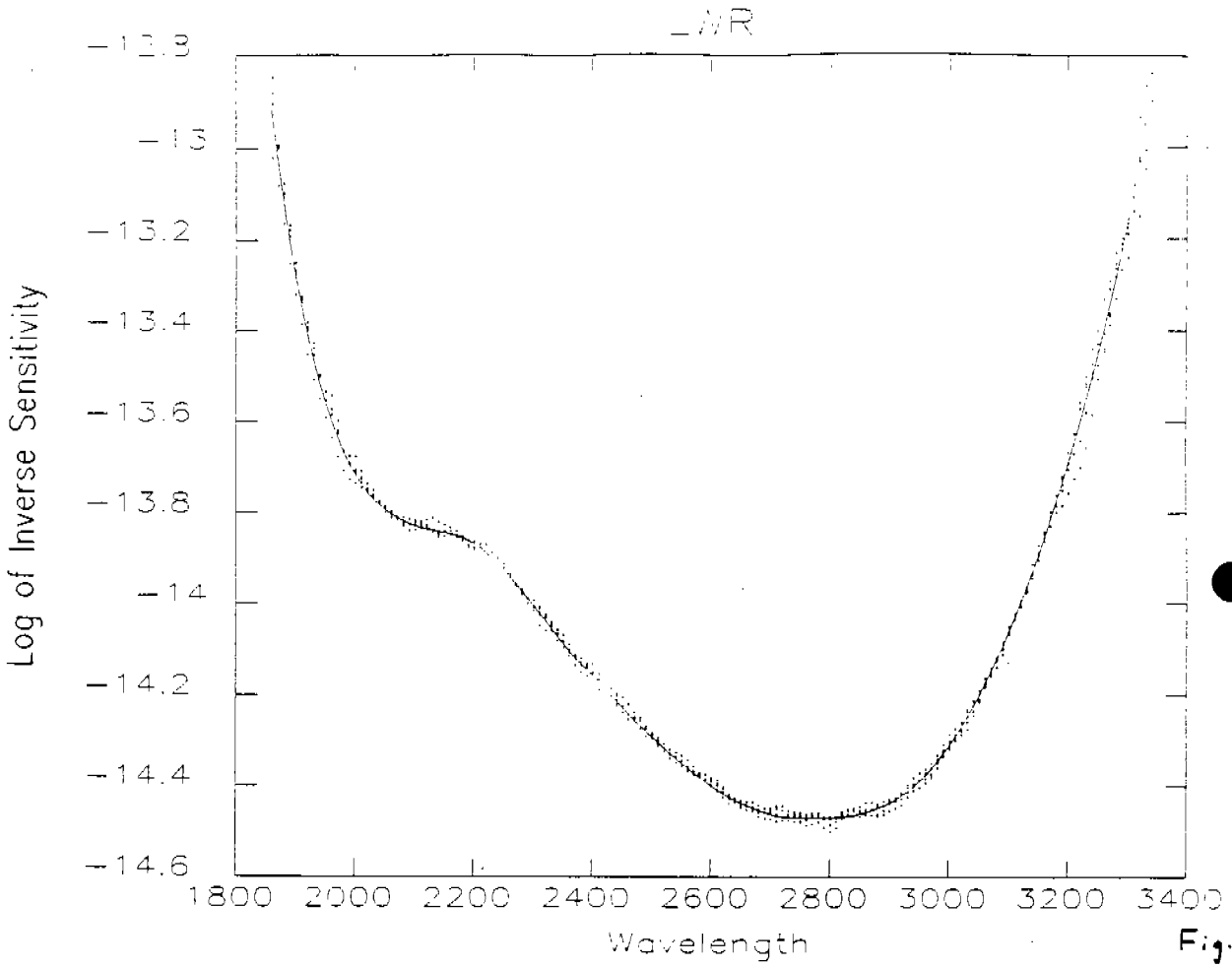
LWR
Log of Inverse Sensitivity
−13.2
−13.4
−13.6
−13.8
−14
−14.2
−14.4
−14.6
1800 2000 2200 2400 2600 2800 3000 3200 3400
Wavelength

Fig. 7

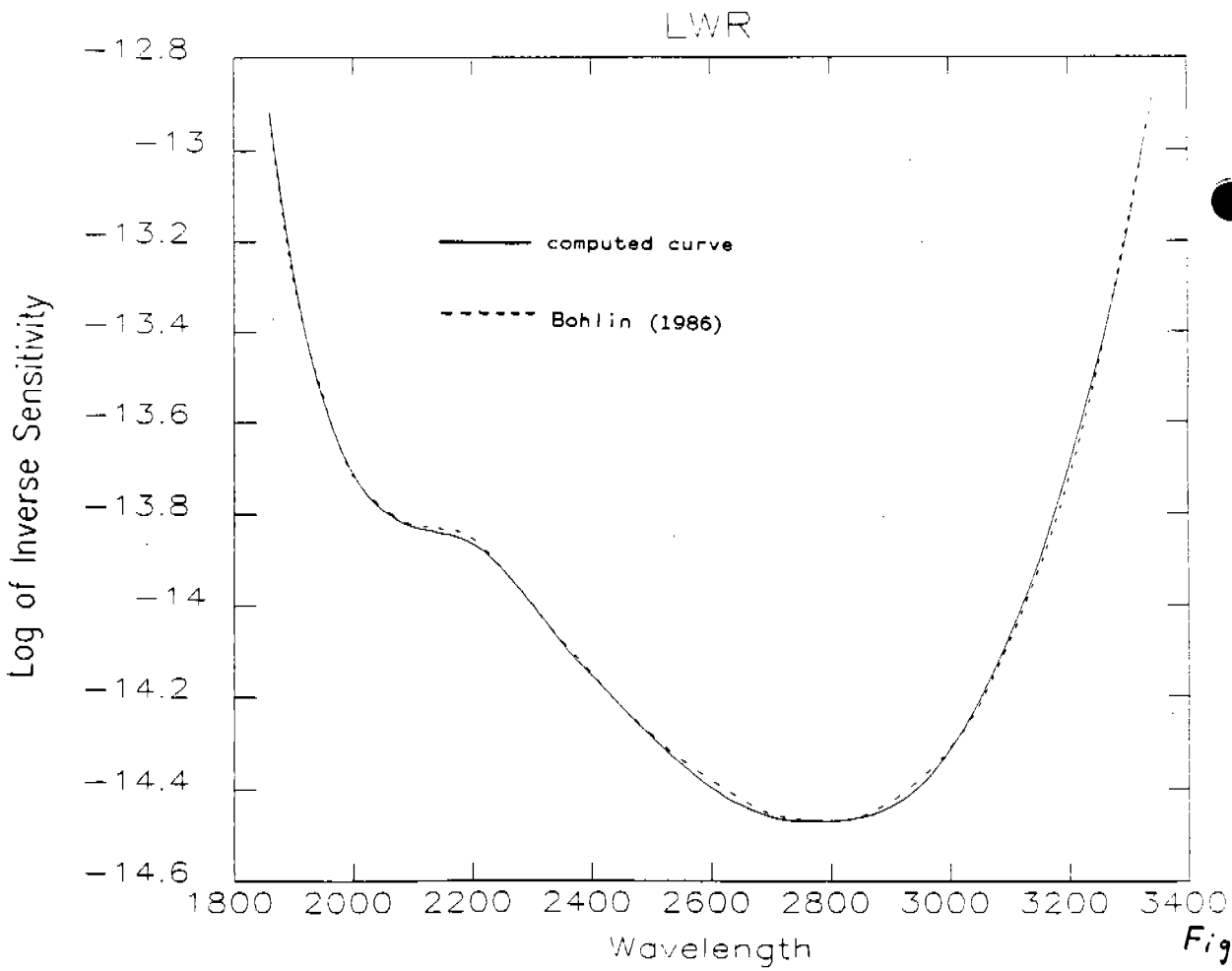
LWR
computed curve
Bohlin (1986)
Log of Inverse Sensitivity
−12.8
−13
−13.2
−13.4
−13.6
−13.8
−14
−14.2
−14.4
−14.6
1800 2000 2200 2400 2600 2800 3000 3200 3400
Wavelength

Fig. 8

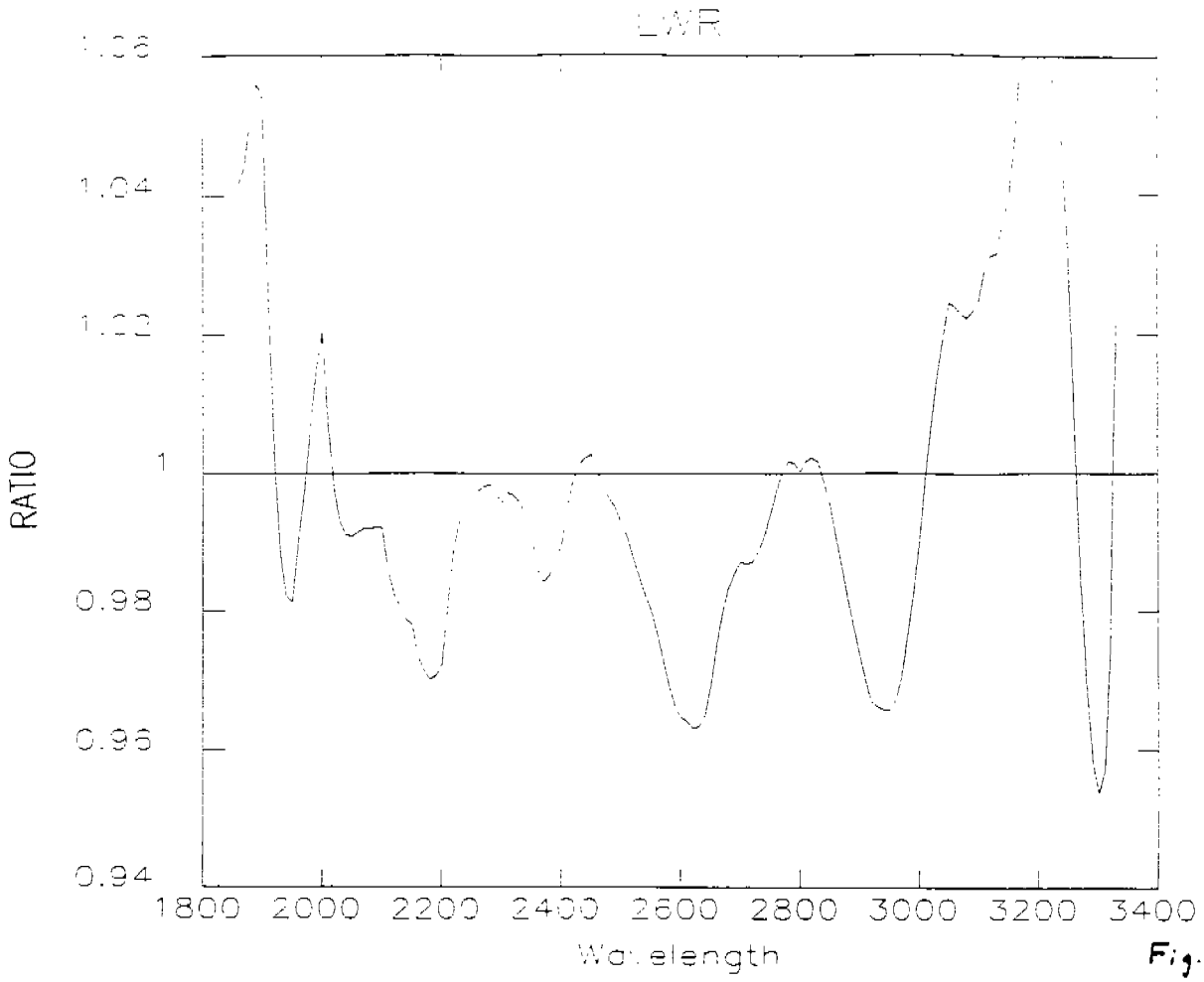
LWR
RATIO
1.08
1.04
1.02
1
0.98
0.96
0.94
1800 2000 2200 2400 2600 2800 3000 3200 3400
Wavelength

Fig. 9

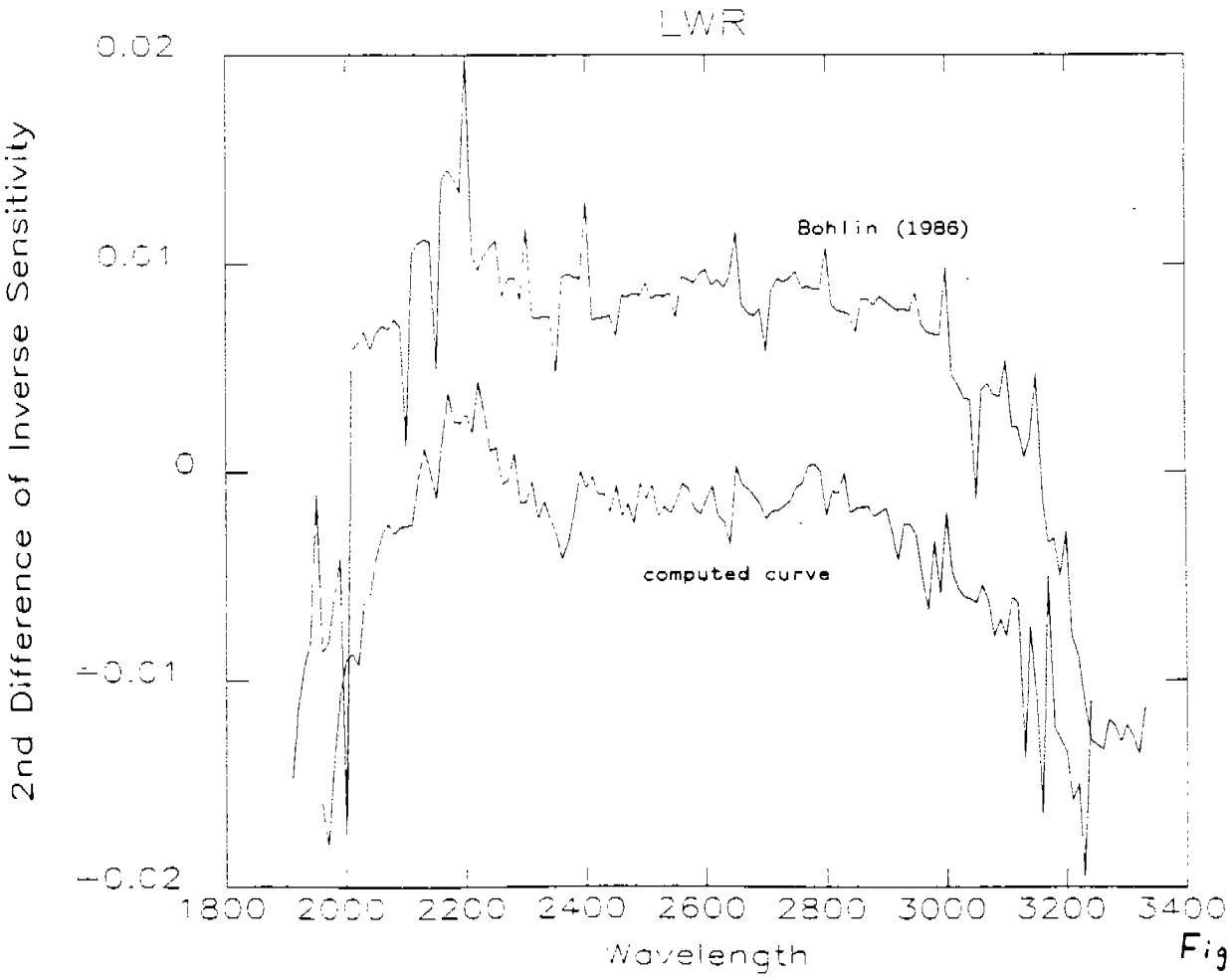
LWR
2nd Difference of Inverse Sensitivity
0.02
0.01
0
-0.01
-0.02
Bohlin (1986)
computed curve
1800 2000 2200 2400 2600 2800 3000 3200 3400
Wavelength

Fig. 10

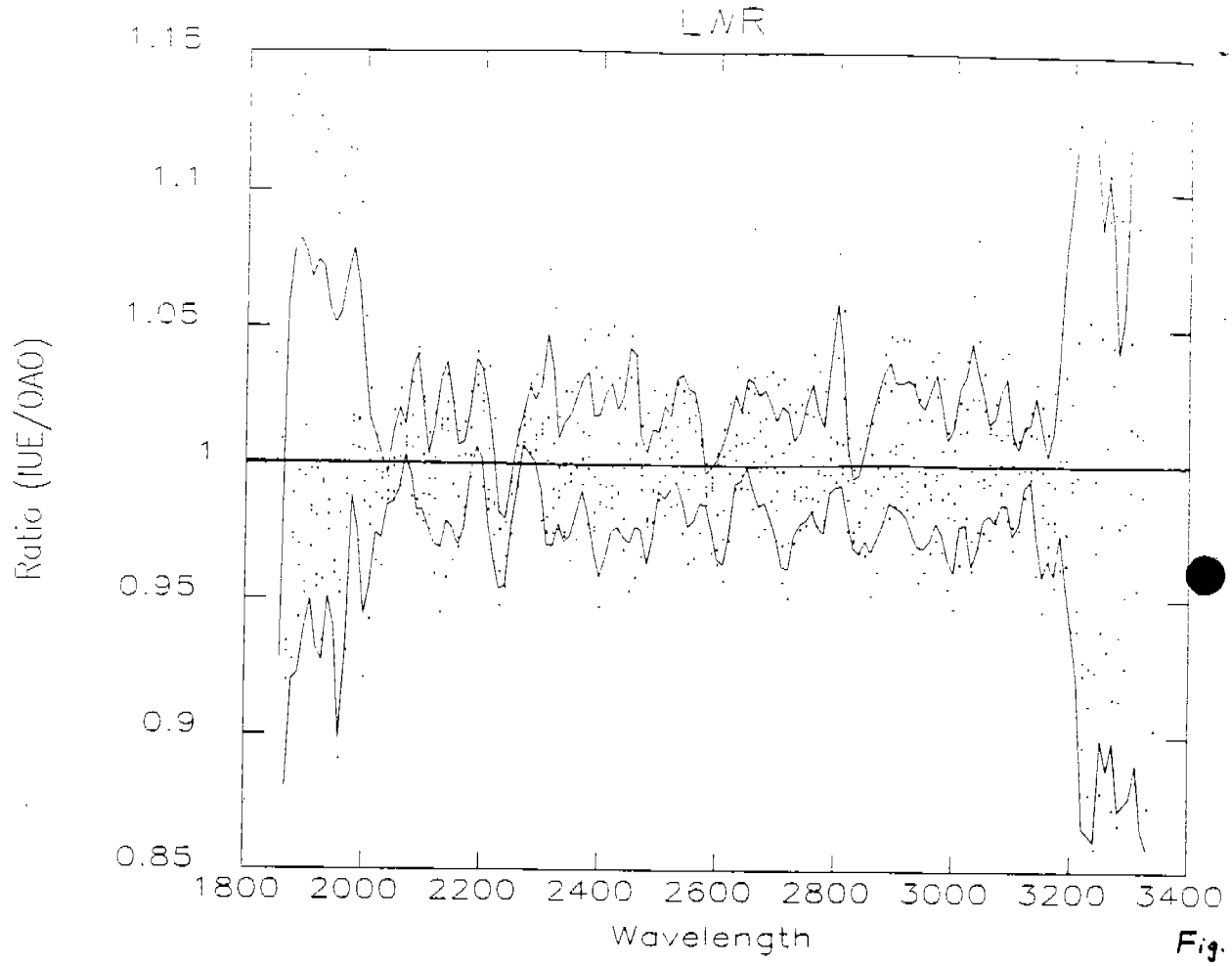
LWR
1.15
1.1
1.05
1
0.95
0.9
0.85
Ratio (IUE/OAO)
1800 2000 2200 2400 2600 2800 3000 3200 3400
Wavelength

Fig.

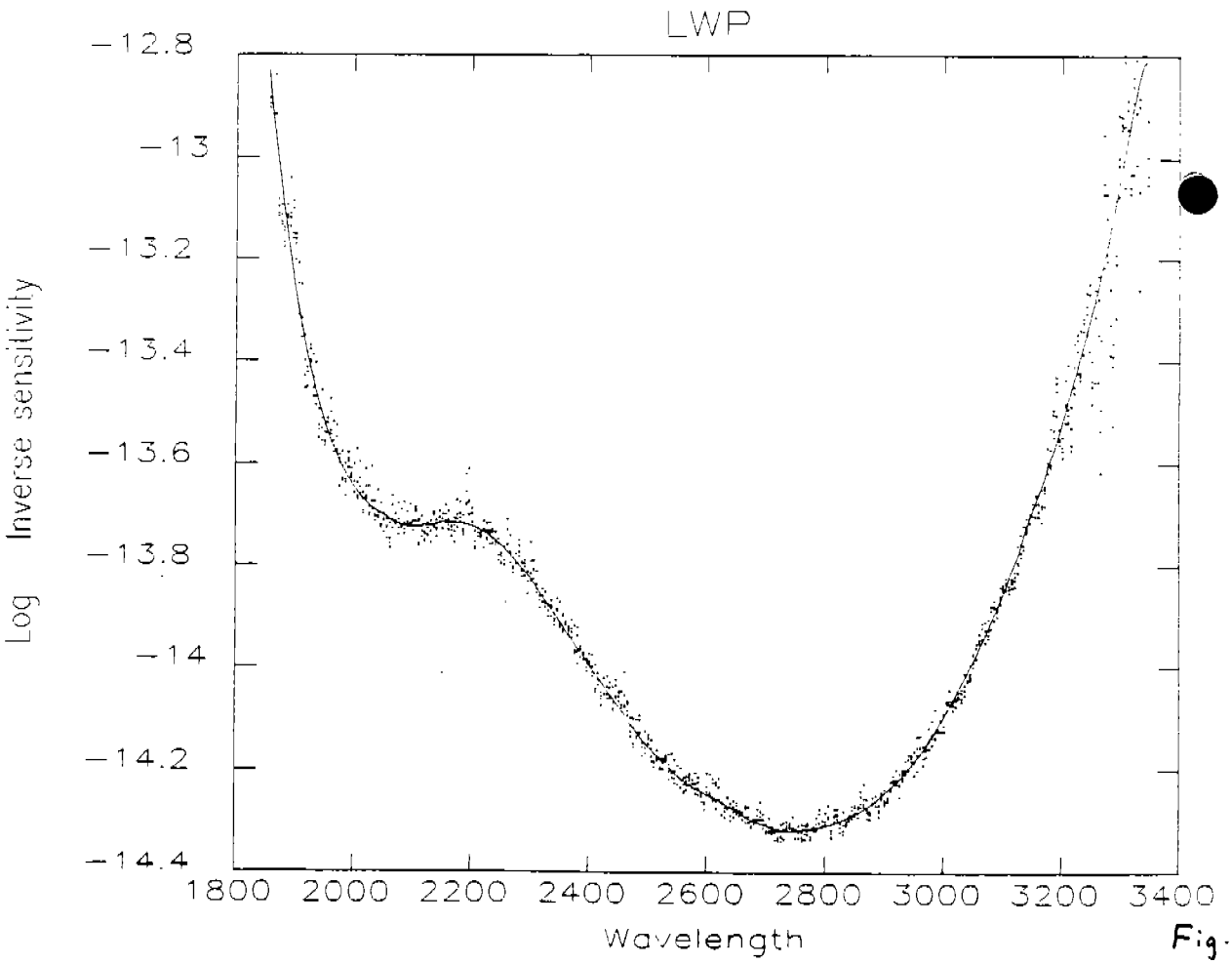
LWP
−12.8
−13
−13.2
−13.4
−13.6
−13.8
−14
−14.2
−14.4
Log Inverse sensitivity
1800 2000 2200 2400 2600 2800 3000 3200 3400
Wavelength

Fig.

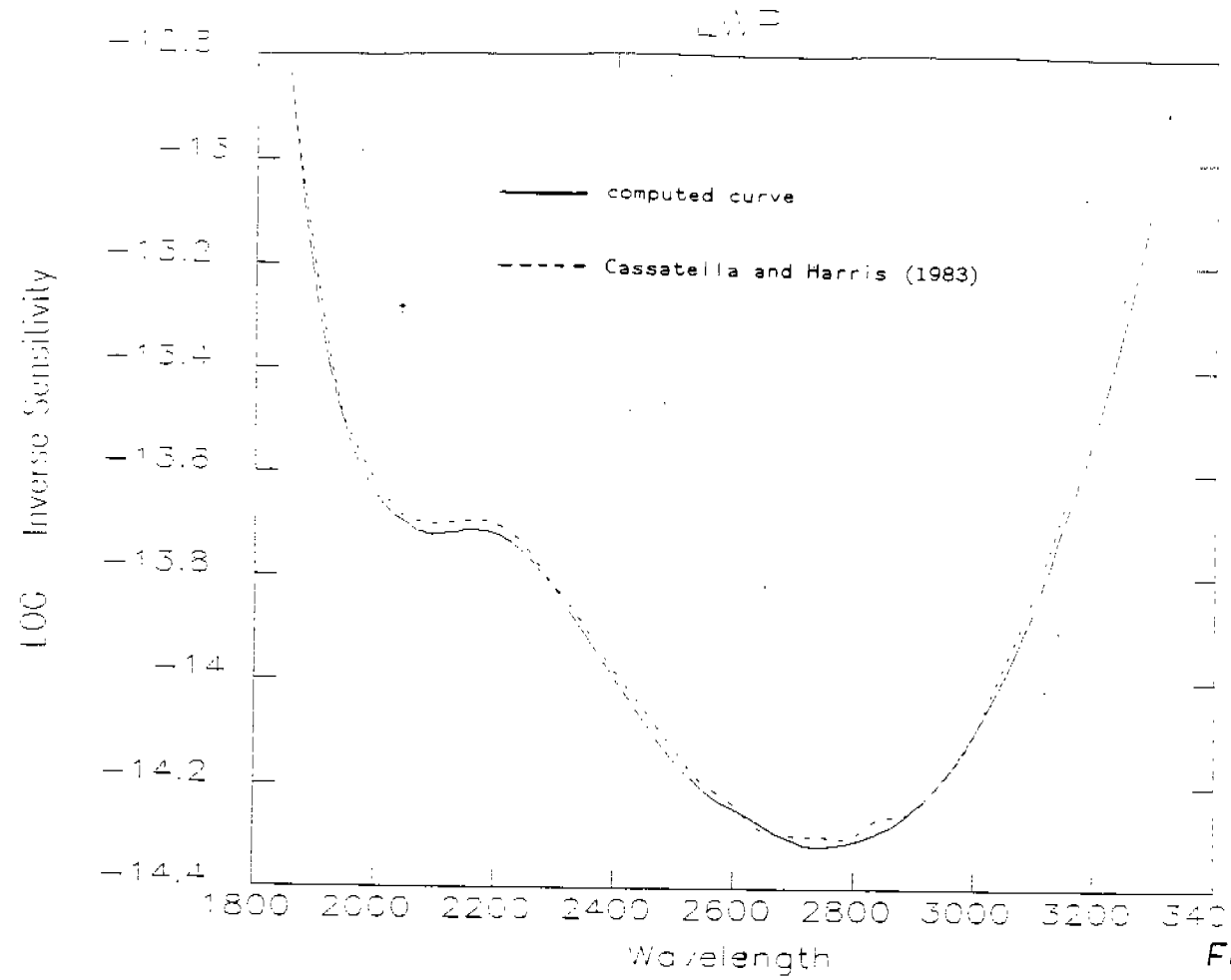
LWP
computed curve
Cassatella and Harris (1983)
LOG Inverse Sensitivity
−13.2
−13.4
−13.6
−13.8
−14
−14.2
−14.4
1800 2000 2200 2400 2600 2800 3000 3200 3400
Wavelength

Fig. 1

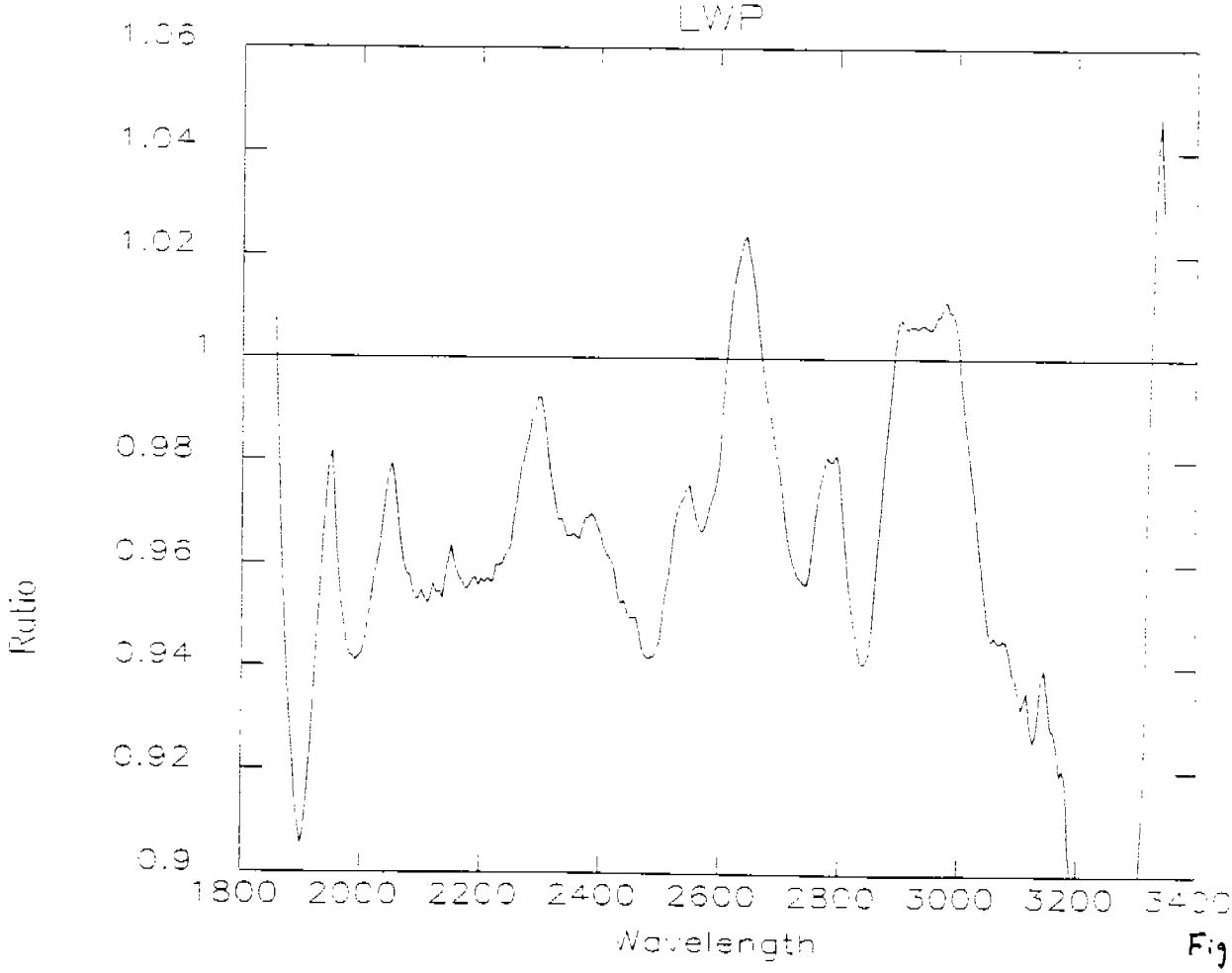
LWP
1.06
1.04
1.02
1
0.98
0.96
0.94
0.92
0.9
Ratio
1800 2000 2200 2400 2600 2800 3000 3200 3400
Wavelength

Fig. 14

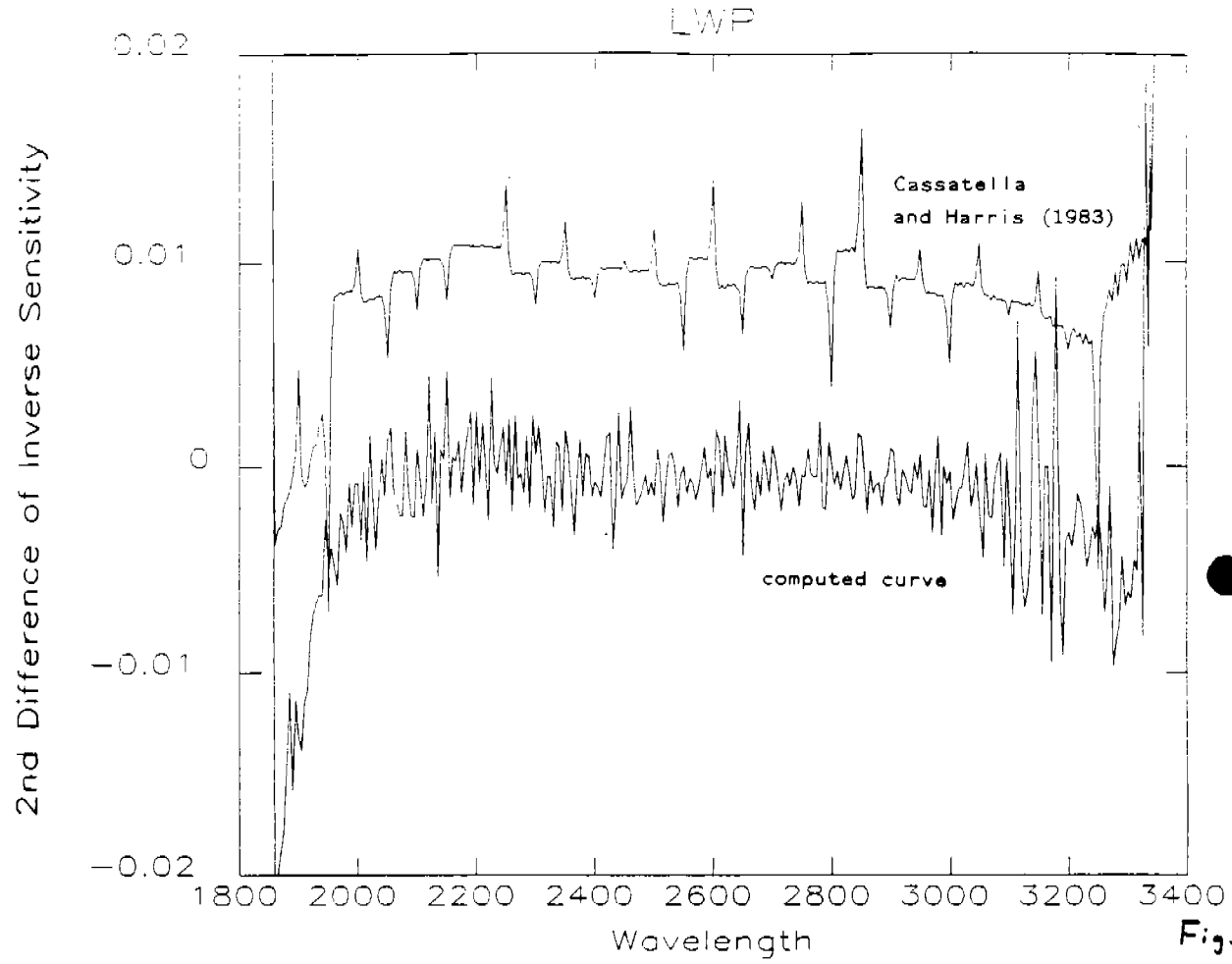
LWP
0.02
0.01
0
−0.01
−0.02
2nd Difference of Inverse Sensitivity
Cassatella
and Harris (1983)
computed curve
1800 2000 2200 2400 2600 2800 3000 3200 3400
Wavelength

Fig.15

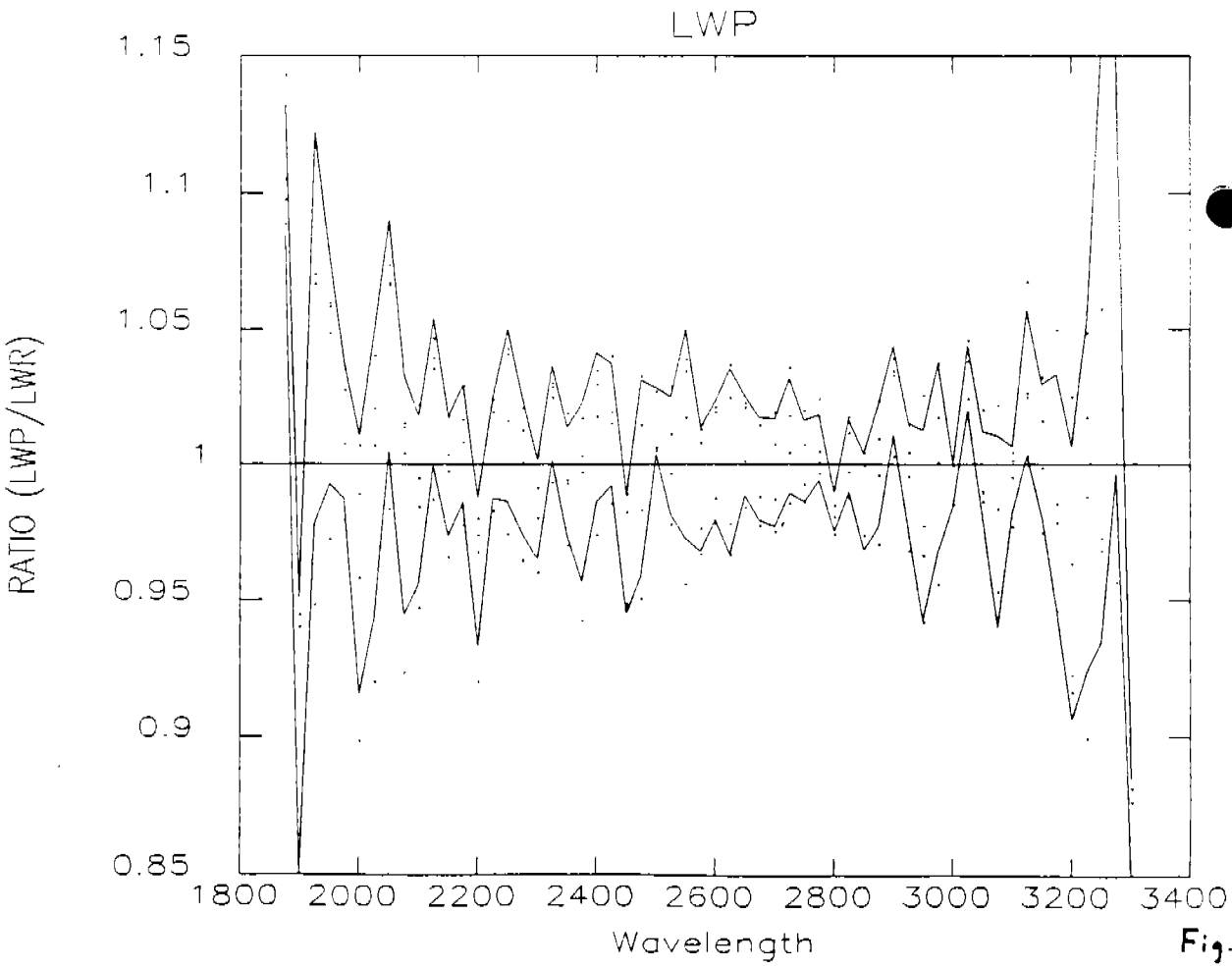
LWP
1.15
1.1
1.05
1
0.95
0.9
0.85
RATIO (LWP/LWR)
1800 2000 2200 2400 2600 2800 3000 3200 3400
Wavelength

Fig.16

APPENDIX A

Software Users Guide

The software for implementation of the algorithms in Section II is coded in Interactive Data Language (IDL). The software modules assume all data has been read into IDL variables and, therefore, makes no assumptions concerning data format. A user should create an IDL driver program to handle the data formats and instrument specific computations to set up the data for the software described below.

STEP 1-- The convolution of the standard star spectrum with the point spread function of the observed spectrum and/or the convolution of the observed spectrum with the point spread function of the standard star spectrum can be handled by the IDL intrinsic routine CONVOL:

```
FLUX = CONVOL(FLUX,PSF)
```

where:

FLUX is the vector of flux values for either spectrum and
PSF is the point spread function interpolated to the same uniform wavelength spacing of FLUX.

If a mean filter is sufficient then the convolution can be performed faster by:

```
FLUX = SMOOTH(FLUX,N)
```

where N is the length in data points of the MEAN filter.

In the case where the point spread function is wavelength dependent or the wavelength scale(s) are significantly non-linear (eg. the FOS prism), no software routine is available to perform the convolution. If step 1 is needed, the user must supply the convolution routine.

STEP 2-- Conversion of the standard star and observed spectra to the same wavelength scales is handled by the routine ABSRATIO:

```
ABSRATIO,WOBS,FOBS,WSS,FSS,MODE,XSTEPS,DELW,WAVE,RATIO
```

where:

WOBS, FOBS - are the observed wavelength and flux arrays smoothed as in step 1.
WSS, FSS - are the standard star's wavelength and flux arrays.

MODE - is the method used to convert FOBS and FSS to the same wavelength scale and can have the following values:

a) 0 - Interpolate FOBS to match the scale of FSS.
b) 1 - Interpolate FSS to match the scale of FOBS.
c) 2 - Integrate FOBS to match the scale of FSS, where the bin size is equal to the sample spacing of FSS.
d) 3 - Integrate FSS to match the scale of FOBS.
e) 4 - Integrate both FSS and FOBS into bins with a specified wavelength interval.

Linear interpolation is used for modes 0 and 1. Trapeziodal integration is used for modes 2, 3, and 4.

XSTEPS - is used for mode 3 only and is primarily for the FOS prism, where WOBS is extremely non-linear. XSTEPS can have a value of 1 (no substepping), 2 (FOS half steps), or 4 (FOS quarter steps). XSTEPS determines the wavelength range covered by each point in FOBS. For XSTEPS=1 the range for FOBS(i) is (WOBS(i)+WOBS(i-1))/2 to (WOBS(i)+WOBS(i+1))/2. For XSTEPS=2 the range is WOBS(i-1) to WOBS(i+1). For XSTEPS=4 the range is WOBS(i-2) to WOBS(i+2). With XSTEPS=1, mode 3 is the inverse of the less general mode 2.

WFIRST - is the starting wavelength for mode 4. If the value is set to zero, the routine selects the first wavelength for you. This parameter is useful, if output wavelengths containing whole numbers are desired.

DELW - is the wavelength bin size for mode 4.

WAVE, RATIO - are the output wavelengths and ratio of the observed flux divided by the standard star flux. Data points where the standard star flux is less than or equal to zero are deleted from the vectors.

ABSRATIO computes a raw (unsmoothed) sensitivity curve. To convert to inverse sensitivity, take the reciprocal of RATIO.

STEP 3-- The computation of the logarithm of the ratio, is done using the IDL system routine ALOG10:

```
C = ALOG10(RATIO)
```

STEP 4-- Smoothing C, is done by the routine DCURVE:

```
DCURVE,C,N,M,NSIG,SMOOTHC,COEFS
```

where:

C - is the ratio from step 3.
N - is the size of the polynomials in data points.
M - is the order of the polynomials.
NSIG - is a parameter which allows rejection of bad data points. After the fit is performed the standard deviation of the residuals from the fit is computed. The data is then refit without using points where the absolute value of the residual is greater than NSIG times the standard deviation of the residuals. In the case of the IUE examples, NSIG was made large enough so that no data points were rejected.
SMOOTHC - is the smoothed curve.
COEFS - is an optional output giving the polynomial coefficients used at each point. COEFS(j,i) is the jth coefficient for point i.

STEP 5--

The inverse sensitivity curve is 10.0 to the SMOOTHC power.